Cellular flows initiate left-right patterning prior to laterality gene expression in amniotes.

Rieko Asai[1,4**], Shubham Sinha[2**], Vivek N. Prakash[2,3,4*], Takashi Mikawa[1*]

[1]Cardiovascular Research Institute, University of California, San Francisco. San Francisco, California 94158, USA. [2]Department of Physics, University of Miami, Coral Gables, Florida 33146, USA. [3]Department of Biology, University of Miami, Coral Gables, Florida 33146, USA. [4]Department of Marine Biology and Ecology, University of Miami, Miami, Florida 33149, USA. [4]Kumamoto University, IRCMS, Kumamoto, 860-0811, Japan.

**Equal contribution

*Corresponding authors: Vivek N. Prakash, Takashi Mikawa

Email: vprakash@miami.edu, takashi.mikawa@ucsf.edu

Author Contributions: RA, TM and VNP conceptualized the project. All authors discussed and wrote the manuscript. RA performed all experiments. SS performed all computational data analysis.

Competing Interest Statement: The authors do not have any competing interests.

Classification: Major: Physical Sciences, Biological Sciences. Minor: Biophysics and Computational Biology; Developmental Biology.

Keywords: Biophysics, Quantitative Biology, Bilateral cellular flows, Particle Image Velocimetry, Midline patterning, L-R asymmetry, Gastrulation, Primitive streak, Cell division

This PDF file includes:

Main Text
Figures 1 to 5
Table 1

Abstract

A bilateral body plan is predominant throughout the animal kingdom. Bilaterality of amniote embryos becomes recognizable as midline morphogenesis begins at gastrulation, bisecting an embryonic field into the left and right sides. Soon after, left-right asymmetry also starts. While a series of laterality genes expressed after the left-right compartmentalization has been extensively studied, the laterality patterning prior to and during midline morphogenesis has remained unclear. Here, through a biophysical quantification in a high spatial and temporal resolution, applied to a chick model system, we show that a large-scale bilateral counter-rotating cell flow, termed as 'polonaise movements', display left-right asymmetries in early gastrulation. This cell movement starts prior to the formation of the primitive streak, which is the earliest midline structure, and earlier than expression of laterality genes. The cell flow speed and vorticity unravel the location and timing of the left-right asymmetries. The bilateral cell flow exhibited a Left side asymmetry at the beginning, but a transition towards Right dominance. Mitotic arrest that diminishes primitive streak formation resulted in changes in the bilateral flow pattern, but the Right dominance persisted. Our data indicate that the left-right asymmetry in amniote gastrula becomes detectable prior to the point when the asymmetric regulation of the laterality signals at the node leads to the left-right patterning. More broadly, our results suggest that physical processes can play an unexpected but significant role in influencing left-right laterality during embryonic development.

Significance Statement

Bilaterians are defined by a bilaterally symmetrical body plan. Vertebrates exhibit external bilateral symmetry but display left-right (LR) asymmetry in their internal organs. In amniote embryos, the initiation of LR symmetry breaking is not well understood. Here, we study LR symmetry breaking in the chick embryo due to its easy accessibility and similarity to human development. Our novel biophysical approaches to quantify cell flows inferred that LR symmetry breaking occurs before the LR genetic patterning programs become detectable. Our work demonstrates that quantitative biophysical parameters can help unravel the initiation of LR symmetry breaking, suggesting an involvement of physical mechanisms in this critical biological patterning process.

Main Text

Introduction

Most animals are classified in the *Bilateria*, possessing a morphological symmetry between the left-right (LR) sides conferred by the midline. Vertebrates present a complex bilateral body plan, displaying bilateral symmetry externally but with asymmetry in the internal organs (1-3). LR patterning and morphogenesis post the asymmetric expression and regulation of the LR regulatory genes, which are expressed after midline morphogenesis, has been extensively studied (4, 5). Although the genetically programmed LR laterality has been extensively studied, LR laterality prior to laterality gene expression has been poorly described.

In amniote embryos, the bilateral body plan becomes recognizable at gastrulation during midline morphogenesis, compartmentalizing the embryonic field into the left and right sides (5, 6). The primitive streak (PS) is the earliest midline structure and serves as a signaling center of gastrulation (7, 8). Prior to and during PS extension, a counter-rotating cell flow, termed as 'polonaise movements', appears at both LR sides along the midline axis (9-15). This bilateral rotating cell flow continues until ingression to generate germ layers starts, at the midline through the PS. At this point, the cell flow shifts from a rotation pattern to a lateral-to-medial pattern toward the midline or PS (16). Previously, we have shown that the lateral-to-medial movements of the epiblast demonstrate ipsilaterality, or side-identity, along the PS (17). Furthermore, a LR-asymmetric membrane potential within the extending PS has been reported (18). These studies hint at a possibility that LR laterality might arise even before the genetically programmed LR patterning is established.

Here, we examine the earliest timing of LR asymmetry patterning in amniote gastrulation. Utilizing computational analyses based on physics of fluids (19), we examined the cellular flows associated with the polonaise movements during early gastrulation in the chick embryo. Visual mapping of biophysical parameters of cellular flows over time revealed that the cell flows on the right side were more dominant than in the left during PS formation. To test the role of midline structure, PS formation was diminished through mitotic arrest. We show that the resulting embryos displayed a shortened duration of bilateral cell flows, however, the LR asymmetry of the flow not only persisted, but the end result was a total right-side dominance of the cell flows. These data suggest that the laterality program is already set up prior to the maturation of the midline initiation of known laterality gene expression, and it does not depend on cell division.

Results

Bilateral flows during early midline morphogenesis in chick gastrulation

To survey the timing of initiation and patterning of bilateral cell flow, we performed live imaging experiments of the early chick gastrulation process, from pre-streak stage until HH3 (Hamburger and Hamilton staging (20)) prior to laterality gene expression (Figure 1 a, b, d) (Methods). To quantitatively analyze the cell flow during early midline morphogenesis or PS formation, the image sequences of fluorescently tagged cells (Methods) were post-processed using the Particle Image Velocimetry (PIV) method (19, 21). PIV is a combined experimental and computational technique from fluid mechanics that is used to quantify time-varying fluid velocity fields by analyzing time-lapse datasets with moving tracer particles (Methods). A snapshot of the flow velocity vectors is shown in Figure (1c), confirming the presence of the well-known polonaise movements in our experiments (Movie 1). To study the details of the time-varying cell flows, for each sample we analyzed the entire image sequence up to 10 hours after the initiation of cellular flows.

To obtain a comprehensive pattern of the bilateral flows, time-averaged data of the flow fields were generated for the entire imaging duration (10 hours) (Figure 1 e-g) (Methods). The time-averaged flow streamlines revealed the intricate structure of two counter-rotating vortices that characterize the bilateral flows (Figure 1e). The time-averaged speed calculations showed that the fastest cell flows were in the peripheral regions of the vortices, on both sides, and were weaker along the Anatomical Midline (Figure 1f). The bilateral flows also had a local rotational component that was quantified using a metric known as vorticity. We extracted the time-averaged vorticity information, and the two counter-rotating vortices were visible in L and R (blue and red respectively) (Figure 1g). The vorticity values considered for further quantification were only those lying inside the embryonic disc (Figure S3). The darker colored regions in L and R (blue and red respectively) are regions with the highest vorticity magnitudes, corresponding exactly to the location of the bilateral vortices.

The full time-averaged analysis provided higher resolution data for spatiotemporal patterning of the bilateral flows. Looking closely at the speed plot (Figure 1f), the regions with higher speed on the R side (yellow and red regions) occupy a slightly larger area than on the L side. Similarly, the vorticity regions in R (red) occupied a larger area than the L (blue) (Figure 1g). These time-averaged results suggest that the bilateral flows may not be fully symmetric. A L-R asymmetry, more specifically a R dominance, became evident (Figure 1 f, g).

Temporal changes in bilateral flows during early midline morphogenesis in chick gastrulation

To study the time-varying bilateral flow patterns in the L and R regions with higher temporal resolution, we performed the PIV averaging at small time intervals by generating hourly time-averaged plots for the entire 10 hours of imaging (Figure 2). Looking at the streamlines, the cell flows initiated in unstable (fluctuating) transient states (0-2 hours) but later developed into two stable counter-rotating vortices (3 hours onwards) (Figure 2). The speed plots showed that the cell flows initiated along the peripheral regions (0-2 hours) and merged at the posterior end. The flows then proceeded from P to A along the Flow Midline (FM) axis (3 hours onwards) (Figure 2). In the next 4 hours (3-7 hours), the L and R sides in the speed plots presented

high symmetry. At later times (7-8 hours), the flow on the R side dominates with a larger area containing higher speeds, and this R domination continues till the end. The streamlines also showed that at later times the R vortex becomes larger in size than the L vortex. The vorticity calculations also showed initial unstable transients (0-2 hours) but stabilized after a few hours (Figure 2). As the bilateral flows proceeded, the L (blue) and R (red) side vortices grew in size to form stable counter-rotating vortices. At a later timepoint (6 hours onwards), the R (red) vortex was getting slightly larger in area compared to the L (blue) vortex. This R side vorticity dominance further increased and persisted till the end.

In another dataset (control sample 2), the bilateral flows initially began with a L dominance and at the end transition to R dominant flows (Figure S1) as seen with other samples. Table 1 lists the origin and the end dominance of flow in all the four control samples in this study. All the cases exhibited R dominant flow at later times. In summary, during early midline morphogenesis, i.e. PS formation during gastrulation in chick embryos, there was a temporal flow transition from L to R dominance pointing that cellular flows generate LR asymmetry.

To test if known laterality genes are detectable at and during LR asymmetry of cell flow as early midline morphogenesis proceeds, the expression patterns of the LR regulatory genes (e.g., *Shh*, *Lefty*, and *Nodal*) were examined during PS extension. At pre-streak stage X [Eyal-Giladi and Kovchav staging (22)], the expression of *Brachyury* (a PS and early mesodermal cell marker) was not detected by in situ hybridization (Figure 3). Upon elongation along the midline, PS cells became distinguishable from other embryonic cells as the area of *Brachyury-positive* (a PS and early mesodermal cell marker) and *Sox3-negative* (an epiblast marker) expression (Figure 3). The PS appears from the posterior marginal zone at HH2 (Figure 3) and anteriorly extends along the midline (Figure 3), until the Hensen's node formed at the anterior tip of the PS at HH4 (20). While the *Brachyury*-expression within the PS was detectable within the extending PS, the LR asymmetric expression pattern of the LR regulatory genes was not evident until Hensen's node formation at HH4 (Figure 3), consistent with previous reports (23-25). Thus, these results suggested that LR asymmetric expression of known laterality genes for the genetically programmed LR patterning is set up later than PS extension. Hence, the cellular flow LR asymmetry initiates LR laterality before midline maturation and laterality gene mediated LR patterning.

Biophysical quantification of bilateral flows during early midline morphogenesis

To quantify the degree of L-R asymmetry, we divided the embryo into L and R sides along a midline axis. We identified three possible midline axes: Anatomical Midline (AM), Biophysical Midline (BM) and Flow Midline (FM). The AM is the line passing through middle of the PS, and BM is the perpendicular bisector to the line connecting the bilateral vortex centers. The FM is the line parallel to the cell flow direction in between the bilateral vortices (Methods) (Figure 4a, Figure S2). To verify if these three midlines coincide with each other, we quantified them over time and measured their angular variation with respect to the vertical (Figure 4b) (Figure S2b). In the analyses that follow, we only retain the cellular bilateral flows inside the circular embryonic disc. The extra-embryonic material surrounding the embryonic disc is stationary, so our quantification methods give rise to results that are noise or artifacts, which will be discarded (Figure S3).

In the initial hours, during the transition, the bilateral flow pattern varied and was unstable between BM and FM. The flow exhibited more stabilized patterns later on, and the angular values of both BM and FM became closer to each other towards the end (Figure 4c) (Figure S2 d, e). The AM showed minimal angular variation in each sample (see Table S3). Figure 4c indicates a larger angular separation between BM and FM in the beginning and their transition to a smaller separation towards the end. The FM was used to separately quantify cell flow dynamics in the L and R sides.

We quantified the speed and vorticity during the bilateral flows in the L and R regions. Both the speed and vorticity plots showed a R dominance towards the end stages (Figure 1 and 2). In addition, the area of both speed and vorticity appeared to be getting larger as embryos develop. To test this possibility, we quantified and compared this area speed and vorticity regions on the L and R sides of the embryo at different

timepoints (see Methods) (Figure 4 d-i) (Figure S4-S5) (Table S2). Figure 4 shows the averaged speed and vorticity area quantification (N = 4 samples). The corresponding area plot for each individual sample is shown in Figure S5. Figure 4d shows the speed quantification heatmap representing speed variations in different regions of cellular flows in the L and R segments. We quantified the change in this speed area in the L and R regions over time and the data show an initial dominance in the L region (Figure 4e). However, as time progresses, this L dominance transitioned towards an R dominance and became amplified at later times. The ratio of R vs L area provides a more comprehensive way to evaluate L-R asymmetry (Figure 4f). The constant line passing through R/L=1 represents the line of perfect symmetry. If the ratio (R/L) is away from 1, this implies a deviation from symmetry (or the magnitude of asymmetry) in the system. Figure 4f shows a L dominance in the beginning which shifted towards an R dominance.

Overall, the ratio (R/L) of area quantification of speeds and vorticity (Figure 4) indicate that the bilateral flows start with a L dominance and end with a R dominance. Hence, our biophysical quantification techniques provided rigorous evidence of the L-R asymmetry that was generated by the bilateral flows.

Bilateral flows in cell-division inhibited embryos during early midline morphogenesis

The above results demonstrate a R dominance of the bilateral flows in control embryos with proper PS extension. It remains unclear, however, how cell flows are induced and patterned bilaterally to the midline or how the R side dominance is regulated. Our recent work has shown that the PS, a key midline landmark tissue, continues to extend and develop even with disrupted cell flows, and that the early phase of the polonaise movements begin bilaterally when PS-extension is diminished by mitotic arrest, i.e. inhibition of cell division (19). However, it is unknown whether laterality of the cell flow would be patterned with defective PS extension along the midline. Here, we investigated this question by carrying out live imaging experiments of the early chick gastrulation process where embryos were treated with aphidicolin, a DNA-polymerase inhibitor. When cell division was inhibited, the PS structure was significantly diminished, consistent with our previous study (19) (Figure S6) (Methods).

In the cell division inhibited embryos, the cell flow patterns were more complicated compared to the control cases and deviated from the bilateral polonaise movements (Figure 5, Movie 2). The flows started with a side dominance (usually R) (Table 1) forming an unstable bilateral flow (Figure 5). This bilateral flow lost stability, and the cell flows merged into one single R vortex at the end. The initial presence of this bilateral flow was not seen in all the cases (Figure S7) (Table 1). However, we observed that in all cases (N = 4), the flows merged to form a single vortex with a R dominance at the end. The temporal evolution of the speeds showed that the cell flows were always R dominant (Figure 5). Similarly, for the vorticity as well, a R dominance was observed from the beginning (clockwise rotating vortex region in red color). The blue regions in the vorticity plots correspond to curved flow regions that have counterclockwise rotations, but a closed vortex did not form (confirmed from the corresponding streamlines) (Figure 5). In these embryos that were under mitotic arrest, the PS formation was diminished, and it was not possible to define an AM. Further, it was not possible to define a consistent BM or FM, because the bilateral flows did not continue until the end. The complexity of cell flows and the inability to define consistent midlines made it difficult to carry out any further biophysical quantification for the embryos under mitotic arrest.

Comparison of bilateral flows in control versus cell-division inhibited embryos during early midline morphogenesis

We summarize the different types of bilateral flows during early midline morphogenesis in chick gastrulation. The time-averaging calculations over the entire duration (10 hours) of our time lapse datasets provide valuable information on the mean cellular movements (Figure 1). However, our results have revealed several temporal flow patterns and variations during the course of 10 hours. To account for these variations, and to compare deviations from bilateral flows, we calculated the half-time averages (5 hours) of the datasets. These half-time averages capture the flow dynamics during the first half (0-5 hours) and the

second half (5-10 hours) of the early midline morphogenesis process in both the control and cell-division inhibited cases, as shown in Figure 6.

Looking at the half-time averaged flows in the control case, in the first half (0-5 hours), the flows were quite symmetric in L and R (Figure 6a). Whereas, in the second half (5-10 hours), the flows became R dominant (Figure 6b). Both the regions of higher speed and vorticity in the R right region were larger than in L, demonstrating that bilateral flows end with a R dominance during early midline morphogenesis (Figure 6a-c). In these embryos, the bilateral flows were accompanied by the formation of the PS structure, and the three distinct midlines (AM, BM, and FM) can be defined, tracked, and quantified.

In the cell division inhibited case, the flows deviated from the classic bilateral mode (Figure 6d-f). The cell flows were R dominant in both the first half (0-5 hours) and the second half (5-10 hours), with a single R vortex forming towards the end. Hence, the cellular flows were always R-dominant in mitosis arrested embryos (Figure 6d-f). In these embryos, the PS structure does not form, and it is not possible to define midlines since these flows are dominated by one single R vortex.

Discussion

Here, we identified previously undetected LR asymmetries in the bilateral cell flows (the polonaise movements) during early midline morphogenesis in chick gastrulation. Our experimental approaches demonstrated that mitotic arrest maintained the cell flows despite diminished PS formation and showed initial bilateral movements that later transitioned to R dominance and a single vortex. These results suggest that PS formation is not crucial for initiating the LR laterality in the cell flows; but is required for stabilizing or maintaining the cell flows particularly at the L side. Our data support a model in which the LR asymmetry in amniote gastrula is already set up, as detected by cell flow patterns, before the genetically programmed LR patterning is established.

It has been assumed that the LR laterality arises in later stages of development, when genetic programs drive LR laterality (4, 23, 26). An implication, based on this model, would be that earlier patterning events, including the bilateral cell flows, are symmetric. However, our results are inconsistent with this assumption. Our study of the bilateral flow with detailed biophysical quantification techniques and novel approaches for time-averaging of cell speeds and vorticity reveals that bilateral flows exhibit LR asymmetry, transitioning from a L dominant flow in the beginning towards R dominant flow at the end.

If the bilateral flows were symmetric, the three midline axes defined here (AM, BM, and FM, Fig. 4 and Fig. S2) were expected to overlap completely. At the onset of the cell flow, there was significant difference in positions for the three midlines. The reason for the high variation is currently unknown but perhaps due to the unstable flow transients in the beginning (first few hours). The angular separation between the midlines starts reducing as the flow becomes stable towards the end, but a small difference persists. These temporal variations in the flow midlines could be an important factor that gives rise to the initial LR asymmetry in the bilateral flows. Our results imply that the emergent flow mechanics that arise from collective cell movements break LR symmetry and impart a LR laterality much earlier than previously expected.

Another unpredicted finding of our study is the R dominance of the flows at the end stages. The signature of the R dominance was seen readily in the control embryos (Figure 2 and 4, Figure S3-S5). In the cell-division inhibited case, the cell flows are highly asymmetric (non-bilateral). The absence of the PS structure may remove or reduce mechanical stability. Consistent with this idea, in some cases, the flows started to develop bilateral-type movements, but ended up merging on one side. In all cases with mitotic arrest, this merging flow was always towards R by forming a single vortex in our data (N=4). This implies that the R dominance already present in control embryos is being further amplified in the mitotic arrest cases. It remains to be explored how the preferred R dominance is induced and or patterned.

Two models have been proposed for establishing the LR laterality in the chick embryo (6, 27). The classic model is that the LR laterality is set up in the blastoderm by localization of maternal determinant before

gastrulation and each LR side develops by following the pre-set pattern(s) (27). The recent model is that molecular signaling(s) from the midline structures, including the PS, initiates and patterns the LR laterality (6) based on extensive genetic and molecular studies (4, 23, 28). Our present study with quantitative biophysical analyses has revealed that the LR asymmetry in the bilateral cell flow appears earlier than establishing the asymmetric expression of the LR regulatory genes (Figure 3). Further, the R dominance in the flow pattern was preserved even though the PS was diminished (Figure 5). These data suggest that the initiation of the cell flow LR laterality is unlikely to depend on the expression of LR patterning genes. It is currently unknown how the cell flow is induced and laterality is patterned, including LR asymmetry. However, at the pre-streak stage, several morphogens (e.g. Wnts and Vg1) are already expressed in the embryonic disc prior to and at the onset of cell flows. Whereas these morphogens are known as axis-inducing factors (29), their roles on the large-scale cell flow, particularly in amniotes, remain to be determined. We have previously demonstrated the ectopic introduction of Vg1 modulates the cell flow pattern (30). Further studies examining any LR asymmetries of these morphogens and/or the response may reveal undefined mechanism(s) of the LR laterality of the cell flow, such as the early symmetry breaking.

While large-scale cell flows during gastrulation are evolutionarily conserved (31-33), the LR laterality of the cell flows remains largely unexplored in most species. Chick embryos begin the cell flow with the bilateral rotating pattern prior to and during early PS extension and then shifts to lateral movement toward the PS after the ingression happens at the midline (34, 35). We have previously reported that the midline structures, including the PS, are required for both LR asymmetry and the ipsilaterality of the lateral cell movements, which subsequently occur after HH3 (17). The current study has demonstrated that mitotic arrest diminished PS formation but the LR laterality in the bilateral rotating cell flow can start (Figure 5 and Figure S7). These findings suggest that the role of the midline structures for the laterality/ipsilaterality of the cell flows would switch in cell flow patterning the early and later developmental windows of the large-scale cell flow.

Whether the LR laterality of the cell flow is related to the later genetically programmed LR patterning remains to be determined. The asymmetric expression of the LR regulatory genes initiates at the Hensen's node (also termed as the 'node' in mice, Figure 3) (23-25). In contrast, the Hensen's node in chick gastrula has the short primary cilia instead the motile cilia (36, 37). These insights suggest that the model of the cilia-regulating gene expression may not be applicable in all amniotes, and alternative models have been proposed (18, 36, 38). Further studies, for example, disruption of the asymmetric counter-rotating cell flow, will clarify the role of the cell flows for the genetically programmed LR patterning. Our study would provide an alternative view for symmetry breaking and provides hints for understanding the establishment of LR laterality and bilateral body patterning.

Materials and Methods

Embryo isolation and culture condition: Fertilized eggs of White Leghorn (Gallus Gallus domesticus) were obtained from a local farm (Petaluma Farms, CA). For ex-ovo manipulations, embryos at pre-streak stage X-XII (22) were isolated from unincubated eggs in Tyrode's solution (137mM NaCl, 2.7 mM KCL, 1mM MgCl2, 1.8mM CaCl2, 0.2 mM Ha2HPO4, 5.5mM D-glucose, pH 7.4) and subsequently cultured until HH3 at 37°C, using the New culture method as previously described for approximately 16 hours (30, 39, 40). After electroporation, the embryos with reagents (described as below) were live imaged on a vitelline membrane stretched around a glass ring according to the New culture method as previously described (30).

Electroporation: Isolated embryos from the yolk were transfected with control-oligo DNA (5'-CCTCTTACCTCAGTTACAATTTATA-3) conjugated with Lissamine (GENE TOOLS) using an electroporator (Nepagene) with 3 pulses of 2.4-3.8 Volts, 50 milliseconds duration, 500 milliseconds interval, and platinum electrodes. The DNA solution delivered to the epiblast contained 0.1% fast green (final 0.02%), 80% glucose (final 4%) and 1mM control-oligo.

Aphidicolin treatment: Aphidicolin (SIGMA, A0781), dissolved in DMSO (SIGMA, B23151), was added to Tyrode's solution to a final concentration of 100μM. The isolated embryos were soaked in Tyrode's solution with either 0.3% DMSO (control), or 100μM aphidicolin for 15 minutes at 37°C. Embryos were then cultured using the New culture method at 37°C.

BrdU assay: Embryos were soaked in Tyrode's solution containing BrdU (final concentration; 0.1mM, Thermo Fisher, B23151) with or without aphidicolin (SIGMA, A0781) at 37°C for 15 minutes, and cultured for 16 hours at 37°C (BrdU was incorporated for 16 hours). Embryos were then fixed in 4% paraformaldehyde (PFA, Electron Microscopy Sciences)/PBS for 30 minutes at room temperature (RT). Embryos were then washed with PBS to remove PFA, and unincorporated BrdU, and incubated with 1M HCl for 1 hour at RT to denature DNA. BrdU signal was detected by immunofluorescence staining with anti-BrdU antibody (1:200, Millipore, MAB3424).

In Situ Hybridization (ISH): After culture, embryos were fixed in 4% paraformaldehyde/PBS at 4C° overnight, then washed in PBT 3 times for 5 minutes each. After hydration and rehydration in methanol in PBT buffers (0% to 100% of methanol), embryos were followed by proteinase K (0.5mg/mL final concentration) in PBT treatment for 2 minutes at RT. Then, the reaction was stopped with glycine (2mg/ml) in PBT for 5 minutes at RT and washed with PBT twice for 5 minutes each. After 2 hours of pre-hybridization in hybridization buffer [Solution I (final concentration: 1% SDS, 5xSSC pH4.5, 50% formamide) with 50μg/mL of yeast tRNA (MilliporeSigma, MA) and 50μg/mL of heparin (MilliporeSigma, MA)], embryos were incubated by probe-containing hybridization buffer at 70°C overnight [probes; *Brachyury*, *Sox3* (a gift from Dr. Raymond B. Runyan), *Slug, Lefty, Nodal, Shh*]. Next day, the buffer was replaced by Solution I, and embryos were washed twice for 30 minutes each. Then, washed twice in Solution III (final concentration: 50% formamide, 2XSSC pH4.5) for 30 minutes each. Followed by TBST wash 3 times for 5 minutes each at RT and blocking with 10% sheep serum in TBST for 2 hours at RT. Antibody-reaction with anti-DIG antibody (1:2000, Roche, MA) was performed at 4°C overnight. Next day, embryos were washed in TBST 5 times for 1 hour at RT, followed by washing in NTMT (final concentration: 100mM of NaCl, 100mM of 50mM MgCl2, 0.1% Triton) twice for 5 minutes. Color development was performed with 4.5μL of NBT and 3.5μL of BCIP in 1mL of NTMT. All ISH were carried out with paralleled control embryos for managing the color development time.

Imaging of chick embryos: The fluorescently tagged embryos were live imaged on Nikon Widefield Epi-fluorescent inverted microscope (Nikon Ti inverted fluorescent Microscope with CSU-W1 large field of view) supported by ANDOR iXon camera or Nikon TIRF/Spinning Disk microscope (Nikon Ti inverted fluorescent Microscope with CSU-22 spinning disc confocal) supported by Prime 95B Scientific CMOS camera at 37C°. After live-imaging, these samples were subsequently performed ISH and imaged by Leica MZ16F microscope with Leica DFC300 Fx camera and Leica FireCam V.3.4.1 software. BrdU-stained samples were imaged on Nikon Ti2 inverted fluorescence microscope supported by a Crest LFOV spinning disk confocal.

Image Processing: Time-lapse imaging datasets from the microscope were opened in the ImageJ (or Fiji) software and split into two channels: brightfield and fluorescence. The brightness and contrast settings of the fluorescence time-lapse images were optimized using suitable thresholds to reduce the noise and enhance the ability to clearly resolve the bright fluorescent markers against a dark background. In the time-lapse sequence, the cellular movements in the embryo only start after a short time delay. For our biophysical motility analysis, we only consider those images after the start of cell movements, this starting point would correspond to the zero time (t), or t = 0 in our analysis. In all the datasets, after determining the starting time, we analyze time-lapse images corresponding to the first 10 hours of early development. This helps make standard time-point comparisons between the different experimental datasets presented here.

Particle Image Velocimetry (PIV): PIV is an experimental technique to quantify fluid flow-fields. This non-intrusive technique is traditionally based on optical time-lapse imaging of tracer particles that are typically illuminated by a high-intensity light source. Next, the time-lapse image sequence is analyzed further and processed using computational algorithms to obtain a spatiotemporal map of flow velocity vectors. Here, we have utilized PIV analysis techniques on the time-lapse images of fluorescently tagged cells in the

embryo to quantify their movements and speeds over time. We employed the MATLAB-based PIVlab package for our data analysis (19)(Supporting Information).

Time averaging of PIV datasets: The PIV analysis by default provides instantaneous velocity vectors that are calculated between two time-points (here this timescale is 3 min). In our datasets, the cell movements over short timescales of 3 mins are very small and the time-resolved transitions in the datasets are inherently noisy due to spatial and temporal fluctuations. Hence, we calculated the time-averaged measurements of the key cell movement parameters (speeds, vorticity) over longer timescales. We found that these time-averaged measurements were significantly better for both detailed quantification and interpretation of asymmetry in the bilateral cell flows. We carried out three different durations of time averaging – (i) 10 hours, (ii) 5 hours, and (iii) 1 hour. This enables interpretation and comparison of bilateral cellular flows at different timescales in the datasets. (i) Time averaging over 10 hours gives an overall picture of the cellular flows during early development. (ii) Time averaged quantification over 5 hours enables us to distinguish between the first half and second half of the process. (iii) Time averaged quantification over 1 hour enables us to carefully study questions about cellular flows such as spatial and temporal origins, changes and transitions, and dominance of L-R asymmetry spanning 10 time-points distributed over every 1 hour. The two key parameters that we use to quantify and characterize cellular flows are speed and vorticity, and we have studied their variation over time during the process of development.

Speed plots: The speed at every spatial point at a given time is calculated as the vector magnitude of the x and y components of the velocities in PIVlab. The cell flow speeds are plotted over a range from 0-2 m/min for all the datasets using a heatmap color scheme continuously varying from low speeds (blue: 0 m/min) to higher speeds (red: 2 m/min).

Streamline plots: Streamlines are the instantaneous and simplified representations of fluid flow directions or paths. Each streamline is tangent to the velocity vector of the fluid flow at every point along its path. They are very helpful in visualizing and analyzing fluid flow. The flow parameters such as vorticity can be better interpreted by comparison with the streamlines. Here, the streamlines were plotted manually with appropriate line width and color. Selecting the “draw streamlines” option in PIVlab and clicking on the vectors automatically generates the most useful streamlines.

Vorticity plots: Vorticity is a vector quantity commonly used in fluid dynamics to quantify the local rotation of a fluid element. Mathematically, the vorticity is calculated as the curl of the fluid velocity. It provides important insights into the rotational regions in the cellular flows, and this rotation can either be clockwise or counterclockwise. High vorticity regions indicate strong local rotation, whereas low vorticity points towards weak rotation. Vorticity plots were generated for all datasets in PIVlab using a heatmap color scheme continuously varying from high clockwise vorticity (red: -5×10^{-3}/min) to 0 (white) to high counterclockwise vorticity (blue: 5×10^{-3}/min).

Biophysical quantification of PIV datasets:
In addition to the default plotting of PIV velocity flow fields and their derived quantities such as speed and vorticity, we further extracted quantitative information to characterize the cell flows in different datasets as described below (Supporting Information).

Midlines: We defined three midlines in the control datasets: AM (defined by the biological structure), BM and FM (defined by the cell flows). The Anatomical Midline (AM) is the line passing through the center of Primitive streak (PS) (Figure 1a). The bilateral flow establishes two counter-rotating vortices in L and R regions. The line drawn perpendicular to the midpoint of the line joining the vortex centers is defined as Biophysical Midline (BM) (Figure S2a). A line drawn parallel to the flow streamlines passing through the midpoint of the vortex centers is defined as the Flow Midline (FM) (Figure S2a) (Supporting Information).

Vorticity and speed thresholds for quantification: For vorticity thresholding, the color map (HSB) scale was set to a minimum value of 1 ($\times 10^{-3}$/min) and maximum value of 5 ($\times 10^{-3}$/min), to retain and quantify 80% of the highest vorticity magnitudes for the L vortex (blue color) (Figure S4b). Since there are two counter-rotating vortices, the 80% threshold for the R vortex (red color) was -1 ($\times 10^{-3}$/min) to -5 ($\times 10^{-3}$/min) (Figure S4b). These threshold scales were kept constant for all the samples (Table S2). Similarly, for speed

thresholding, the thresholding values were set to retain 80% of the highest speeds. The color map (jet) was set differently for different samples (Table S2) (Figure S4a).

Vorticity and speed, area analysis: For vorticity calculations, the coordinates of FM calculated above were used to divide each vorticity matrix into L and R regions. The L contains blue vortex regions whereas the R region contains red vortex regions. Next, in each region thresholding is carried out to pick up only the vorticity above a certain value as described above (Table S2). After this step, the only remaining vectors left were those belonging to the vortex region. Sometimes, these vortices were connected with the peripheral artifacts, so a best guess had to be made to separate it from the artifact. The number of grids containing the vorticity values above this threshold were counted for the two regions. This number was used to denote the area of the L and R vortices. This vorticity area ratio of R/L is plotted in Figure 4i. A similar analysis was performed for all the speed area calculations (Figure 4d-f). The quantification was performed for all hourly averaged time points of vorticity and speed for a sample. This provided the quantitative time evolution information of speed and vorticity in the different datasets, and a comparison between L and R regions (Figure 4).

Acknowledgments

We thank present and past Mikawa lab and Prakash lab members for their invaluable suggestions and/or assistance. This work was supported in part by grants from NIH (R01HL122375, R37HL078921, R01HL132832, R01HL148125) to T.M.; Uehara Memorial Foundation Fellowship and JSPS Postdoctoral Fellowship for Research Abroad to R.A.; University of Miami for startup funding support to V.P.N.

Figures and Tables

Table 1. Features of bilateral flows in control versus aphidicolin-treated embryos.

Sample Number	Origin of flows in L-R, initial dominance	Duration of Bilateral flows	Flows toward end stages in L-R, end dominance	End dominance starting time
Control Sample 1	L	0 - 10 hr	R	7-8 hr
Control Sample 2	L	0 - 10 hr	R	7-8 hr
Control Sample 3	L	0 - 10 hr	R	not clear
Control Sample 4	R	0 - 10 hr	R	always
Aphidicolin Sample 1	R (left vortex forms)	No bilateral flow, vortex direction switches	R	6-7 hr
Aphidicolin Sample 2	R	No bilateral flow	R	Always
Aphidicolin Sample 3	R	0 - 7 hr	R	Always
Aphidicolin Sample 4	R	No bilateral flow	R	always

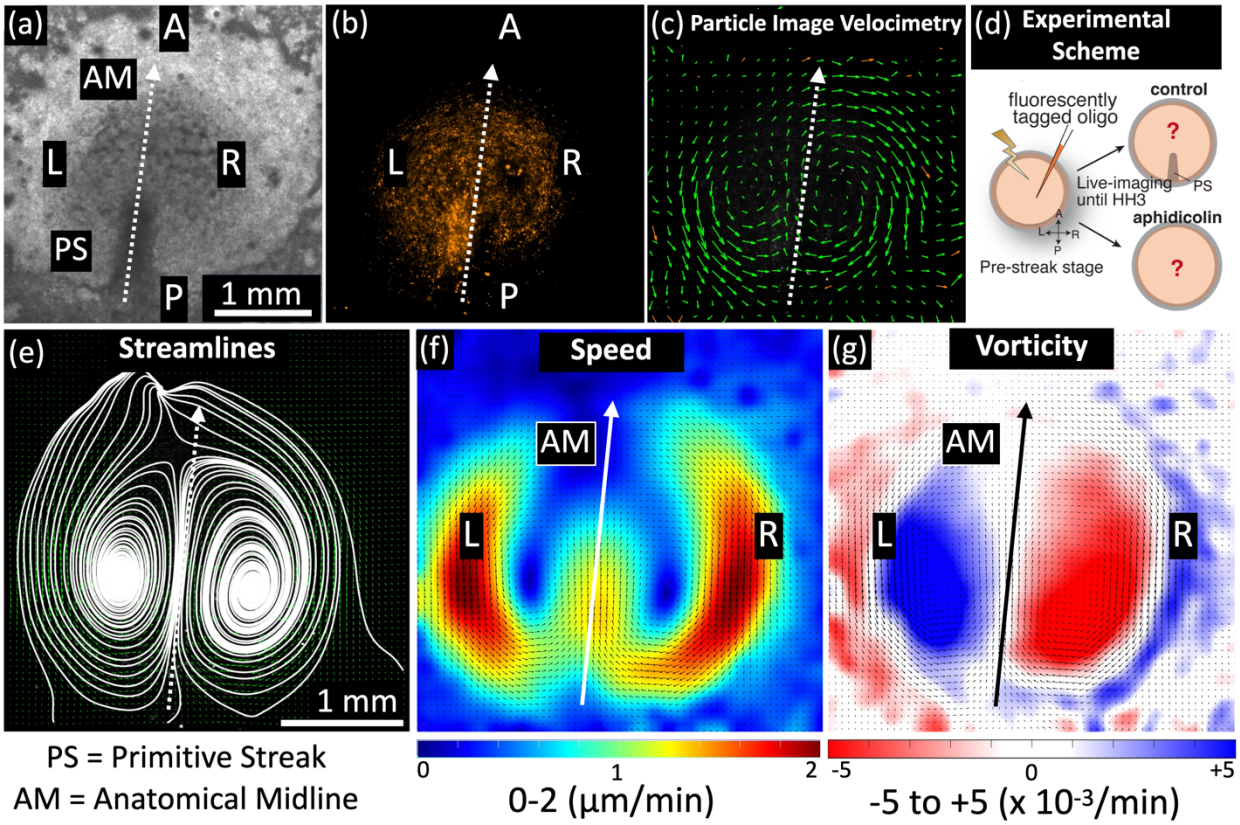

Figure 1: Cellular flows during early chick embryo development. Upper panel: (a) Brightfield image of chicken embryo gastrulation showing development of Primitive Streak (PS) at the midline (at stage HH3). The Anatomical Midline (AM) defined by the PS is shown in dotted lines, and the Anterior (A), Posterior (P), Left (L) and Right (R) regions are also labeled. The images shown in (a-c) correspond to the time point of 10 hours post initiation of cellular motion in control sample 1 (see Table 1). (b) Fluorescence image of the embryo revealing cells tagged with fluorescent markers. (c) Results from Particle Image Velocimetry (PIV) analysis (Methods), the green arrows represent instantaneous velocity vector fields. (d) A schematic showing the experimental scheme (Methods). **Lower panel:** (e-g) Time-averaged (over 10 hours) results from PIV analysis. (e) Streamlines reveal bilateral cellular flow patterns with counter-rotating vortices in both L and R regions. (f) Cellular speeds: heat map indicates lowest speeds in blue color and highest speeds in red color. (g) Vorticity (measurement of rotation): Red colors indicate clockwise rotation and blue colors indicate counterclockwise rotation directions. Both speed and vorticity plots show slightly higher magnitudes on the Right side, indicating asymmetry in the bilateral flows (f, g). The length scale bar shown in (a) is the same for panels (a-c), and length scale bar in (e) is the same for panels (e-g).

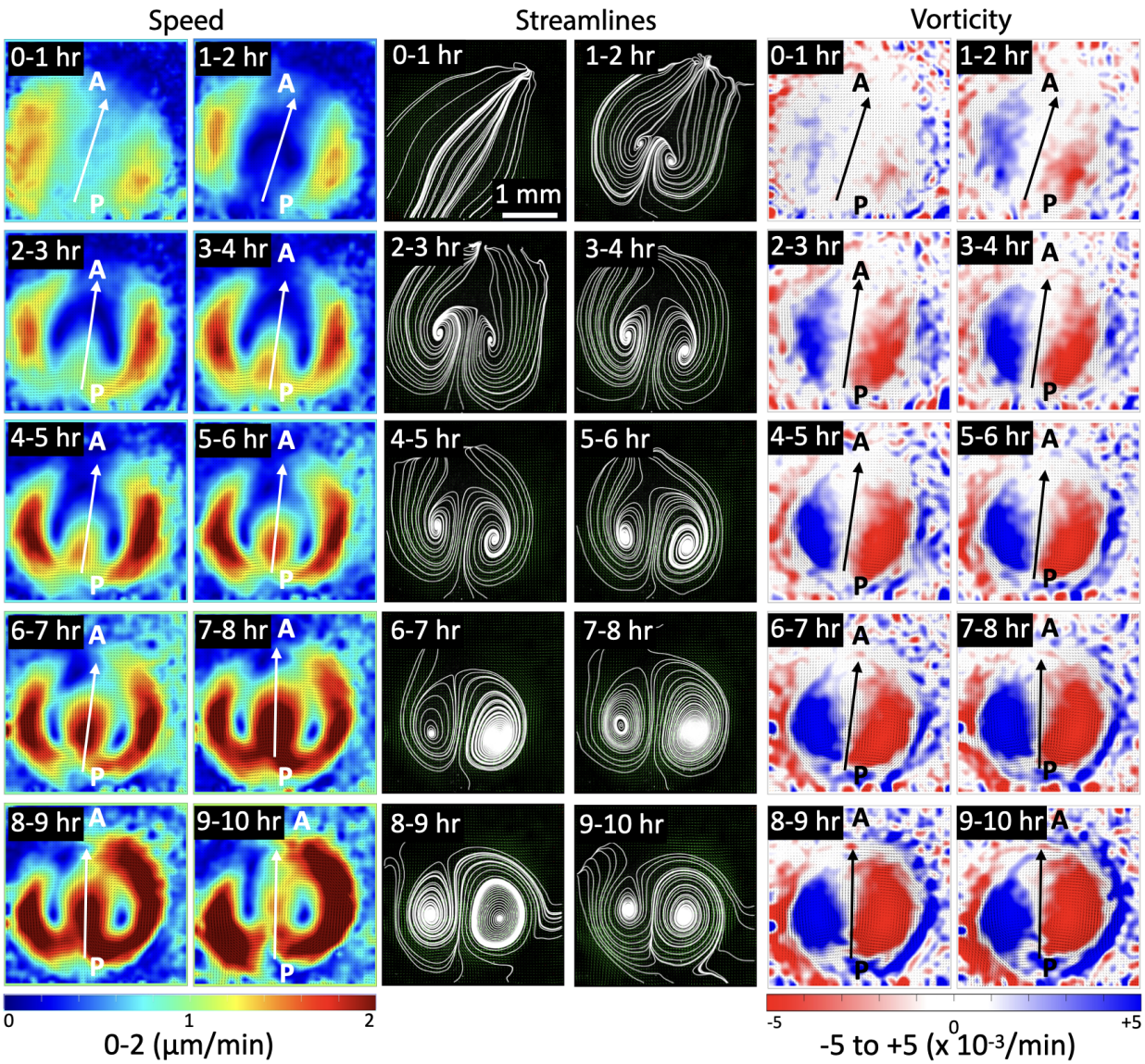

Figure 2: Temporal progression of bilateral flows during early chick embryo development. Short time-averaged (1 hour) sequences of (a) speed, (b) streamlines, and (c) vorticity from PIV analysis of control sample 1 (see Table 1). (a) Speed: cellular flows show initial speed transients (0-2 hours), which later stabilize and lead to symmetric L-R speed patterns (2-7 hours). This symmetry in flow speed is lost at the later stages (7 hours onwards) and cellular speeds become R dominant. (b) Streamlines: Cellular flows initiate only at the sides (0-1 hours), and then progress in the midline region displayed by the bilateral transients (1-3 hours). Later these bilateral flows form two stable counter-rotating vortices (3 hours onwards). (c) Vorticity: Initial flow transients (0-2 hours) stabilize to form symmetric bilateral flows (2-7 hours) with well-defined counter-rotating vortices (blue-red colors). Following this (7 hours onwards), the L-R symmetry is lost, with the R vortex increasing in dominance. The arrows represent the Flow Midlines (FM) and indicate direction of flows at that location (Methods). The length scale bar shown in the first streamline panel (0-1 hour) is the same for all panels.

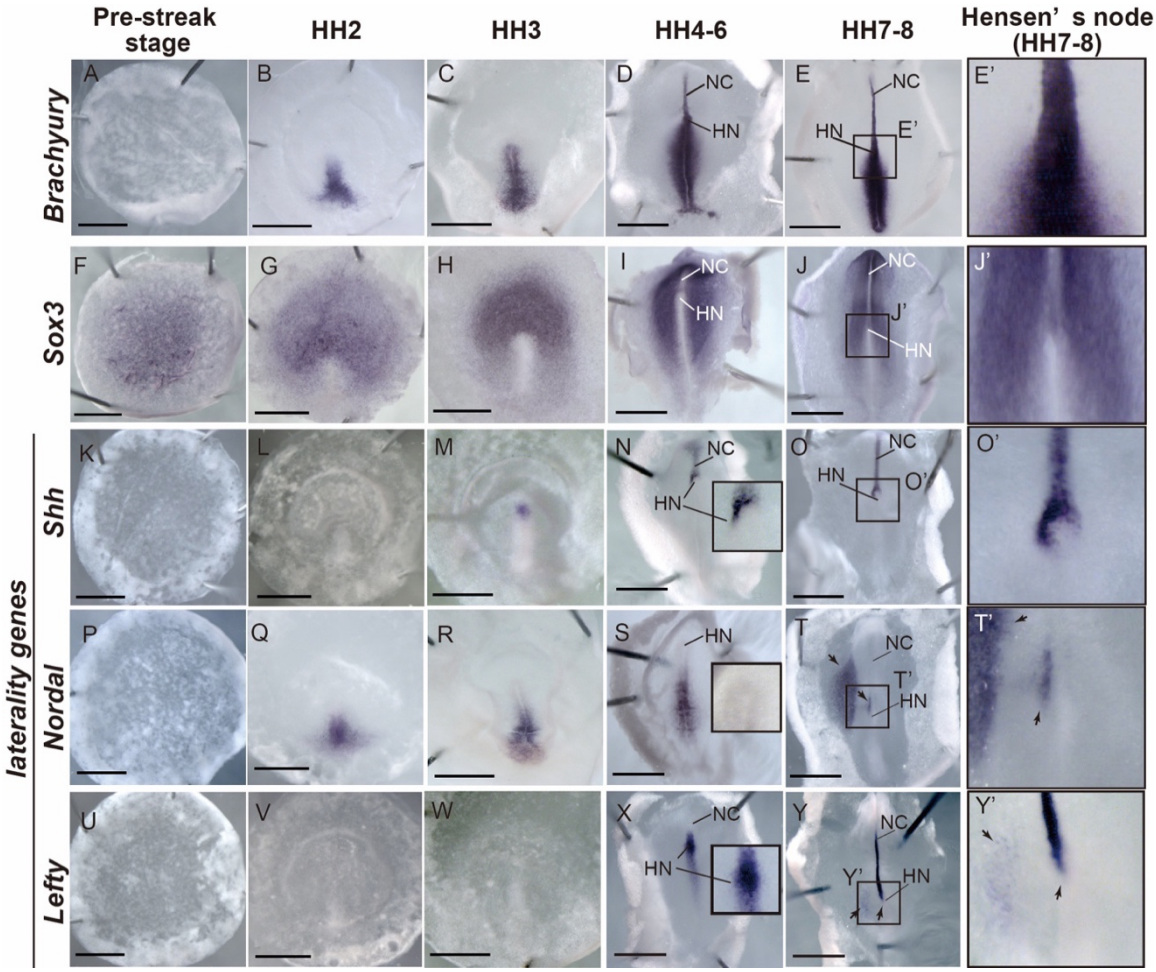

Figure 3: Laterality genes exhibit left-right asymmetric expression pattern after HH4.
(A-Y') Pre-streak stage to HH8 whole mount in situ hybridization of Brachyury (A-E'), Sox3 (F-J'), Shh (K-O'), Nodal (P-T'), Lefty (U-Y'). (E', J', O', T', Y') Enlarged Hensen's node in (E), (J), (O), (T), (Y), respectively. Black arrows indicate left-right asymmetric expression pattern. Scale bars, 1mm.

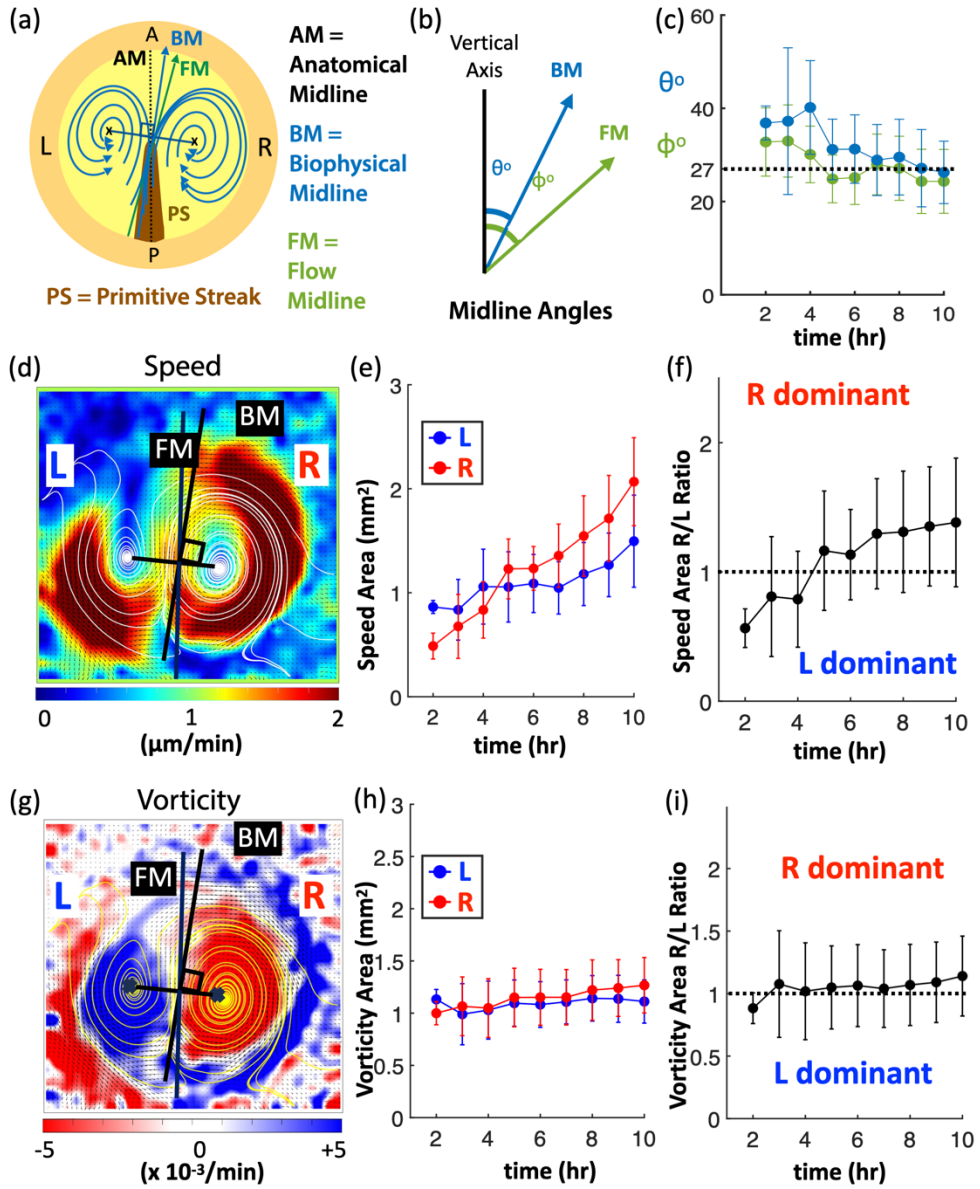

Figure 4: Biophysical quantification of bilateral flows over time. (a) Cartoon representation of bilateral flows accompanied by Primitive Streak (PS) formation. The three different midline axes are shown: AM, BM, and FM (supplementary information). (b) The angle subtended by FM and BM to the vertical axis (c) The averaged (N = 4 samples) mean angles of BM and FM for the control samples. The dotted black line shows the constant angle maintained by AM with the vertical axis. (d) Quantification of cell speeds with the L and R regions separated by the FM. (e) The averaged mean (N = 4 samples) of L and R speed area of control samples. (f) Time evolution of the ratio of mean speed area of R vs L (R/L values obtained from panel e). (g) Vorticity in L and R regions (blue and red respectively) considered for vorticity area quantification. (h) Temporal evolution of average of vorticity area (N = 4 samples) in L and R regions. (i) Ratio of R vs L vorticity area (from panel h). The error bars in all plots represents the standard error.

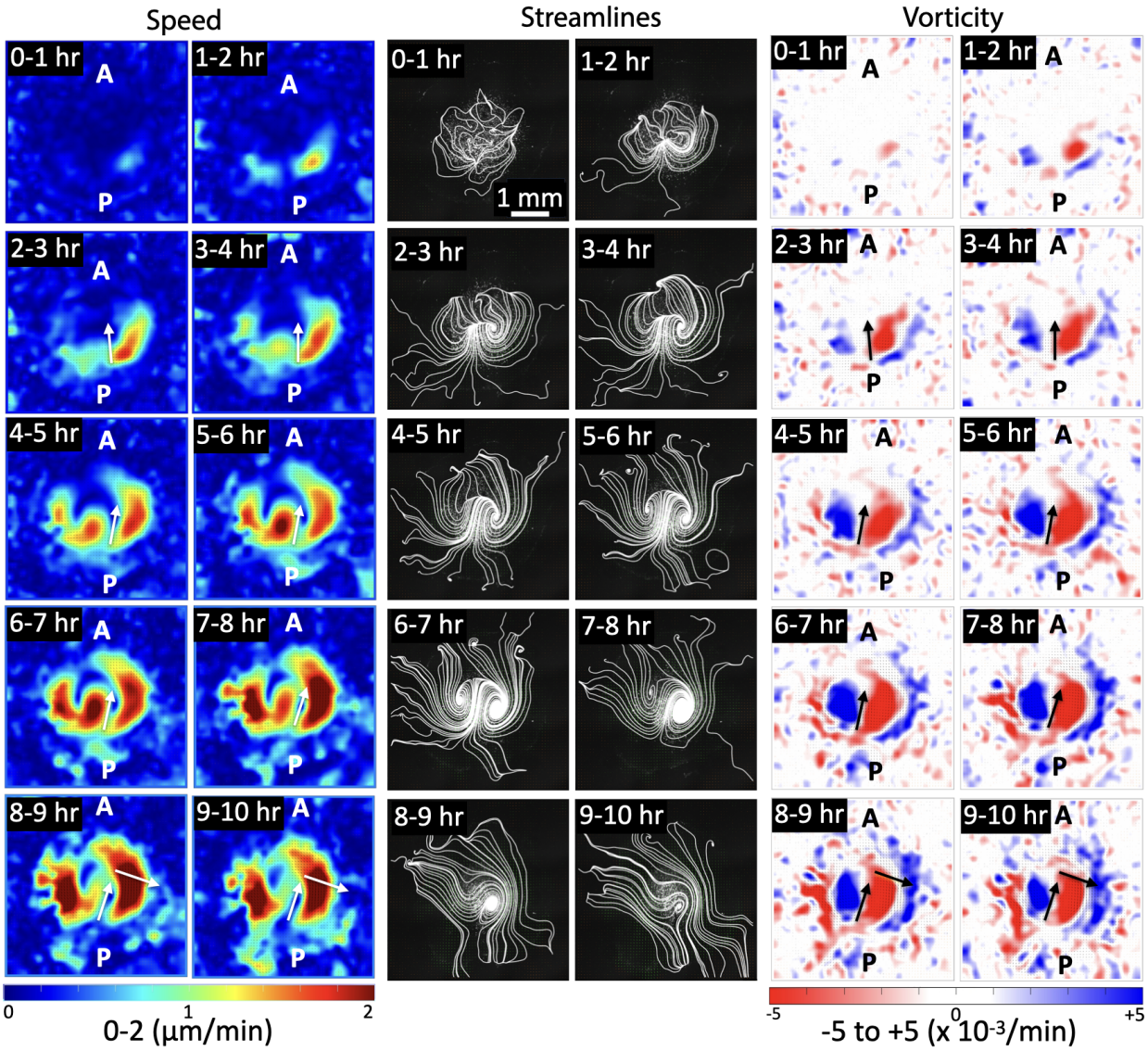

Figure 5: Time evolution of flows in cell-division inhibited chick embryos. Short time-averaged (1 hour) sequences of (a) speeds, (b) streamlines, and (c) vorticity from PIV analysis of aphidicolin sample 3 (see Table 1). (a) Speed: Cellular flows are initially transient and first start on the R side (0-2 hours). These transients stabilize without any L-R symmetry with a dominant R side pattern until the end (2-10 hours). (b) Streamlines: The initial cellular flow transients are random (0-2 hours), but following these bilateral flows develop (2-7 hours). Subsequently, the flows lose L-R symmetry and turn into a single vortex on the R side (7-10 hours). (c) Vorticity: initial flow transients (0-2 hours) develop to form bilateral flows (2-7 hours) with well-defined counter rotating vortices (blue-red colors). After this (7 hours onwards) even though there is only a R vortex present (red), the blue color indicates the counterclockwise rotational regions that still persist (but do not form a closed vortex) (Methods). The short arrows serve as a guide to indicate direction of flows at that location, but do not represent midlines (Methods). The length scale bar shown in the first streamline panel (0-1 hour) is the same for all panels.

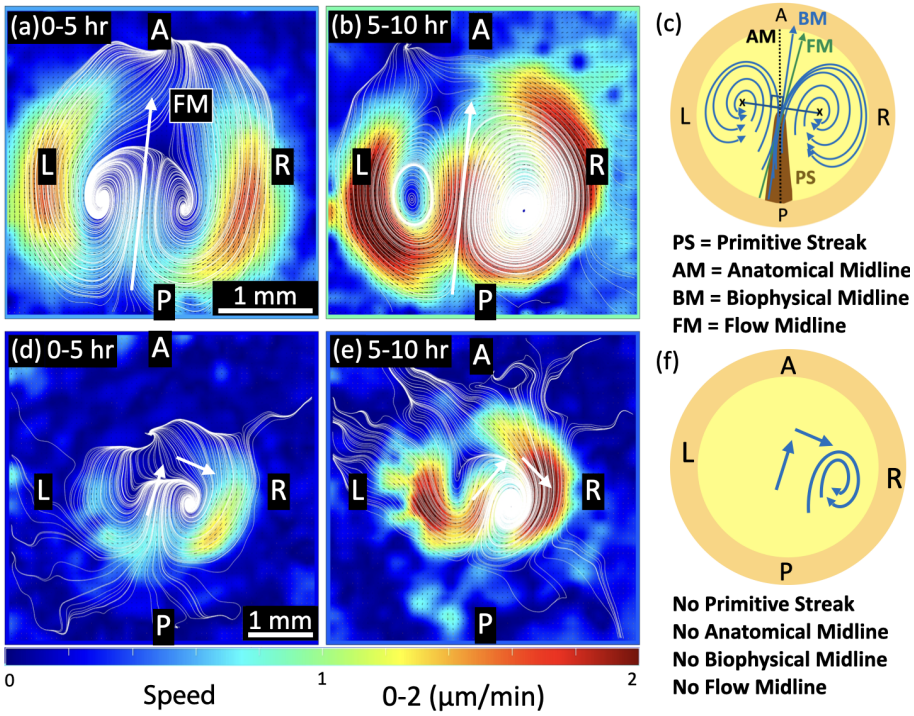

Figure 6: Comparison of cellular flows in early chicken embryo development: control vs cell division inhibited. Time-averaged (5 hour) speed results from PIV analysis of control & aphidicolin (see Table 1). **Top panels – control embryo** (control sample 1, Table 1): (a) During the initial period (0-5 hours), the bilateral flows have a high degree of L-R symmetry. (b) In the later period (5-10 hours), the bilateral flows may still be maintained but the L-R symmetry is lost and the R dominance is visible. (c) Cartoon representation of bilateral flows in the control, with flows more dominant in R. The PS forms but the AM and BM axes may have a slight deviation from each other. **Bottom panels – cell-division inhibited embryos** (aphidicolin sample 3, Table 1): (d) During the initial period (0-5 hours), there is a single vortex formation on the R side. (e) In the later period (5-10 hours), the single R vortex persists and dominates the flow speeds. (f) Cartoon representation of flows in cell-division inhibited embryos, with single R vortex dominated flows. The PS does not form, and the midlines AM, BM, and FM are all absent. The short arrows serve as a guide to indicate direction of flows at that location, but do not represent midlines (Methods). The length scale bar shown in (a) is the same for (b), and the length scale bar shown in (d) is the same for (e).

References

1. M. Q. Martindale, J. R. Finnerty, J. Q. Henry, The Radiata and the evolutionary origins of the bilaterian body plan. *Molecular Phylogenetics and Evolution* **24**, 358-365 (2002).
2. E. K. Namigai, N. J. Kenny, S. M. Shimeld, Right across the tree of life: the evolution of left-right asymmetry in the Bilateria. *Genesis* **52**, 458-470 (2014).
3. J. P. Richter, R. C. Bell, *The Notebooks of Leonardo Da Vinci* (Dover Publications, 1970).
4. C. J. Tabin, The key to left-right asymmetry. *Cell* **127**, 27-32 (2006).
5. M. Levin, N. Nascone, Two molecular models of initial left-right asymmetry generation. *Med Hypotheses* **49**, 429-435 (1997).
6. N. A. Brown, L. Wolpert, The development of handedness in left/right asymmetry. *Development* **109**, 1-9 (1990).
7. M. Chuai *et al.*, Cell movement during chick primitive streak formation. *Dev Biol* **296**, 137-149 (2006).
8. M. Saadaoui, D. Rocancourt, J. Roussel, F. Corson, J. Gros, A tensile ring drives tissue flows to shape the gastrulating amniote embryo. *Science* **367**, 453-458 (2020).
9. J. Firmino, D. Rocancourt, M. Saadaoui, C. Moreau, J. Gros, Cell Division Drives Epithelial Cell Rearrangements during Gastrulation in Chick. *Dev Cell* **36**, 249-261 (2016).
10. G. Serrano Najera, C. J. Weijer, Cellular processes driving gastrulation in the avian embryo. *Mech Dev* **163**, 103624 (2020).
11. L. Bodenstein, C. D. Stern, Formation of the chick primitive streak as studied in computer simulations. *Journal of Theoretical Biology* **233.2**, 253-269 (2005).
12. S. A. Sandersius, M. Chuai, C. J. Weijer, T. J. Newman, A 'chemotactic dipole' mechanism for large-scale vortex motion during primitive streak formation in the chick embryo. *Phys Biol* **8**, 045008 (2011).
13. B. Vasiev, A. Balter, M. Chaplain, J. A. Glazier, C. J. Weijer, Modeling gastrulation in the chick embryo: formation of the primitive streak. *PLoS One* **5**, e10571 (2010).
14. M. Serra *et al.*, A mechanochemical model recapitulates distinct vertebrate gastrulation modes. *Sci Adv* **9**, eadh8152 (2023).
15. M. Chuai, G. Serrano Nájera, M. Serra, L. Mahadevan, C. J. Weijer, Reconstruction of distinct vertebrate gastrulation modes via modulation of key cell behaviors in the chick embryo. *Sci Adv* **9**, eabn5429 (2023).
16. O. Voiculescu, L. Bodenstein, I. J. Lau, C. D. Stern, Local cell interactions and self-amplifying individual cell ingression drive amniote gastrulation. *Elife* **3**, e01817 (2014).
17. L. Maya-Ramos, T. Mikawa, Programmed cell death along the midline axis patterns ipsilaterality in gastrulation. *Science* **367**, 197-200 (2020).
18. D. S. Adams *et al.*, Early, H+-V-ATPase-dependent proton flux is necessary for consistent left-right patterning of non-mammalian vertebrates. *Development* **133**, 1657-1671 (2006).
19. E. Stamhuis, and William Thielicke, PIVlab – Towards User-friendly, Affordable and Accurate Digital Particle Image Velocimetry in MATLAB. *Journal of open research software* **2.1** (2014).
20. V. Hamburger, H. L. Hamilton, A series of normal stages in the development of the chick embryo. 1951. *Dev Dyn* **195**, 231-272 (1992).
21. W. Thielicke, Sonntag, R., Particle Image Velocimetry for MATLAB: Accuracy and enhanced algorithms in PIVlab. *Journal of Open Research Software* (2021).

22. H. Eyal-Giladi, S. Kochav, From cleavage to primitive streak formation: a complementary normal table and a new look at the first stages of the development of the chick. I. General morphology. *Dev Biol* **49**, 321-337 (1976).
23. M. Levin, R. L. Johnson, C. D. Stern, M. Kuehn, C. Tabin, A molecular pathway determining left-right asymmetry in chick embryogenesis. *Cell* **82**, 803-814 (1995).
24. K. Katsu, D. Tokumori, N. Tatsumi, A. Suzuki, Y. Yokouchi, BMP inhibition by DAN in Hensen's node is a critical step for the establishment of left-right asymmetry in the chick embryo. *Dev Biol* **363**, 15-26 (2012).
25. T. Mikawa, A. M. Poh, K. A. Kelly, Y. Ishii, D. E. Reese, Induction and patterning of the primitive streak, an organizing center of gastrulation in the amniote. *Dev Dyn* **229**, 422-432 (2004).
26. T. Nakamura, H. Hamada, Left-right patterning: conserved and divergent mechanisms. *Development* **139**, 3257-3262 (2012).
27. H. Wilhelmi, Experimentelle Untersuchungen über Situs inversus viscerum. *Archiv für Entwicklungsmechanik der Organismen* **48**, 517-532 (1921).
28. S. M. Pagán-Westphal, C. J. Tabin, The transfer of left-right positional information during chick embryogenesis. *Cell* **93**, 25-35 (1998).
29. S. B. Shah *et al.*, Misexpression of chick Vg1 in the marginal zone induces primitive streak formation. *Development* **124**, 5127-5138 (1997).
30. R. Asai, V. N. Prakash, S. Sinha, M. Prakash, T. Mikawa, Coupling and uncoupling of midline morphogenesis and cell flow in amniote gastrulation. *eLife* 10.7554/eLife.89948.2, 12:RP89948 (2023).
31. S. F. Gilbert, M. J. F. Barresi, *Developmental Biology* (Oxford University Press, 2017).
32. L. Solnica-Krezel, D. S. Sepich, Gastrulation: making and shaping germ layers. *Annu Rev Cell Dev Biol* **28**, 687-717 (2012).
33. M. Leptin, Gastrulation movements: the logic and the nuts and bolts. *Dev Cell* **8**, 305-320 (2005).
34. R. Wetzel, Untersuchungen am Hühnchen. Die Entwicklung des Keims während der ersten beiden Bruttage. *Wilhelm Roux Arch Entwickl Mech Org* **119**, 188-321 (1929).
35. L. Gräper, Die Primitiventwicklung des Hühnchens nach stereokinematographischen Untersuchungen, kontrolliert durch vitale Farbmarkierung und verglichen mit der Entwicklung anderer Wirbeltiere. *Wilhelm Roux Arch Entwickl Mech Org* **116**, 382-429 (1929).
36. L. A. Stephen *et al.*, The chicken left right organizer has nonmotile cilia which are lost in a stage-dependent manner in the talpid(3) ciliopathy. *Genesis* **52**, 600-613 (2014).
37. J. Männer, Does an equivalent of the "ventral node" exist in chick embryos? A scanning electron microscopic study. *Anat Embryol (Berl)* **203**, 481-490 (2001).
38. J. Gros, K. Feistel, C. Viebahn, M. Blum, C. J. Tabin, Cell movements at Hensen's node establish left/right asymmetric gene expression in the chick. *Science* **324**, 941-944 (2009).
39. R. Asai, M. Bressan, T. Mikawa, Avians as a Model System of Vascular Development. *Methods Mol Biol* **2206**, 103-127 (2021).
40. D. A. T. New, A New Technique for the Cultivation of the Chick Embryo in vitro. *Journal of Embryology and Experimental Morphology* **3**, 326-331 (1955).